Romanian Reports in Physics, Vol. 68, No. 4, P. 1523–1535, 2016

SPECTROSCOPIC MEASUREMENT TECHNIQUES TO CHARACTERIZE THE BONES OF RATS TREATED IN HYPERBARIC CHAMBER

M. VASILE[1*], F. LAMONACA[2], A. NASTRO[3], V. CIUPINA[4], D. NEAMTU[5]

[1] "Ovidius" University of Constanta, Medical School, Romania
[2] University of Sannio, Department of Engineering, Italy
[3] University of Calabria, Department of Chemical and Chemical Technologies, Italy
[4] "Ovidius" University of Constanta, Faculty of Applied Sciences and Engineering
[5] National Institute of Endocrinology C.I. Parhon, Bucharest, Romania
**Corresponding author*: mvasile@univ-ovidius.ro

Received May 20, 2015

Abstract. There are a lot of publications on bone structure characterisation of the biomaterials used as prosthesis. This work deals with the physicochemical characterisation of the rat bone tissue harvested from the specimens treated in hyperbaric chamber, using X-ray diffraction, scanning electron microscopy, and high resolution solid state ^{31}P-NMR and ^{13}C-NMR. The bone samples from the rat forelimbs, grafted with a pastille of MCPM/CC, were harvested from the rats treated with oxygen in a hyperbaric chamber. The measurements on posterior limbs of the reference rats are used as control.

Key words: rat bones, crystallinity, X-ray, NMR analysis, hyperbaric chamber, morphology.

1. INTRODUCTION

The bone tissue is a variety of connective tissues constituted of cells (osteoblasts, osteocytes, and osteoclasts), collagen fibres and intercellular substances (amorphous or fundamental). The mineralization of the extracellular matrix confers a remarkable resistance and hardness to the bone.

The intercellular substance has two components: the organic and the inorganic matrices. The organic matrix is composed of collagen fibres attached to an amorphous substance being composed of protein–mucoid-polysaccharide, glycosaminoglycan or proteoglycan complexes, and glycoproteins.

The inorganic matrix is essentially composed of calcium phosphates, calcium carbonate, and minor amounts of other salts. The combination between inorganic constituents (responsible for the hardness and rigidity) and organic

constituents (responsible for the resistance to the traction and pressure) associated to the internal organisation of the bones are to the origin of the bone mechanical properties.

The bones have their essential role to support the body, protecting in its cavities, the inserted organs. They constitute the passive organs of the movement, functioning as levers of force, resistance or displacement, on which muscles are acting during the body movements [1]. The bones give the insertion of the muscles by the tendons, protect the internal organs contained in the cranial and chest cavity and are host of the marrow hematopoietic elements.

In addition to these functions, the bone tissue plays an important role in the body metabolism because it represents a calcium bank, from which the ions can be mobilised for the homeostatic regulation of their concentration in the blood and in other body liquids [2]. From the morphological point of view, two types of bones can be distinguished: spongy and compact. The spongy or trabecular bone is constituted of a tri-dimensional network of "spicules", lattice of thin threads of bones, called "trabeculae", building the pillars of strength delimiting a labyrinth of interconnecting spaces occupied by the bone marrow.

In 1998, Rho *et al*. have studied the mechanical properties of the bones, both at the micro- and nano-structure level [3]. Timonen *et al*. (1998) have introduced the Nuclear Magnetic Resonance (NMR) in the characterisation of the bones. In their study is included the application of the micro images for the tri-dimensional characterisation of the "trabecular" bone [4]. In 2005 Legrand *et al*. have published a work on the biomaterials used as prosthesis. The techniques used to characterise these biomaterials are essentially the X-ray diffraction (XDR) and the Nuclear Magnetic Resonance (^{31}P-NMR) [5]. In 2000, Bohic *et al*. have introduced these techniques together with the Fourier Transform Infrared Spectrometry (FTIR) to characterise the rat bones [17].

The low crystallinity of the inorganic part at the amorphous limit of the bones is the reason that the bone is elastic and not fragile [1–5, 17–20].

Many scientists utilized instrumental technique to characterize and evaluate the properties of the bones [18–20]. Also, recently it was proposed the utilization of thermal analysis (TA), thermogravimetry (TG), and differential scanning calorimetry (DSC) to characterize the human bones. The efforts are devoted to obtain an objective diagnosis [6–15].

The aim of this study is to characterise from physicochemical point of view the rat bone tissue treated by hyperbaric oxygen by usual procedures used for humans [21]. The spectroscopic characterisation has been done using X-ray diffraction, scanning electron microscopy, and high resolution solid state ^{31}P-NMR.

2. MATERIALS AND METHODS

2.1. EXPERIMENTAL PROTOCOL

The rats (*Rattus norvegicus*) were kept in a cylindrical hyperbaric chamber with a certification ISPSEL (diameter 270 mm, length 560 mm) for 90 min, 100 % oxygen at 2.4 ATA (total absolute pressure, the equivalent of diving to 45 feet underneath the seawater) 5 days a week for 4 weeks. The pressure inside the chamber was no higher than 2.4 ATA.

The following samples of the forelimbs of the rat were studied:

- Control rat bones
- Bones of rats treated in hyperbaric chamber
- Grafted bones of rats treated in hyperbaric chambers.

The grafts have been prepared with a mixture of mono-calcium-phosphate monohydrate (MCPM, Ca $(H_2PO_4)_2$) (Aldrich, USA) and calcium carbonate (CC, $CaCO_3$) (Carlo Erba, Italy) powders, in the stoichiometric mole ratio 1:2.5 to obtain a Ca/P ratio of about 1.67, a value typical for hydroxyapatite [22].

The rats were divided in two groups: first study group made of 6 grafted rats (GR) and second study group made by 6 rats grafted and treated in hyperbaric chamber (GR+HBC). The graft was been just on the anterior limbs of each rat. Their posterior limbs without graft are only used as a control.

The removed members of the rats were prepared for the study by washing them with a physiological solution during 30 days to remove the lipoid residues. They were successively cleaned and then broken into big pieces and, finally, they were put again in acetone for 2–3 days. The cleaning with acetone allowed us to avoid the decomposition of the material and, at the same time, to get bone fraction completely free of lipids.

3. CHARACTERISATION

The XDR gives information on the characteristics and diagnostic of the materials that are either industrial or natural, in form of single crystals, aggregation of small crystallites, blocks of metals, etc. [23].

The instrument used is a Philips 1730/10 diffractometer equipped with a vertical goniometer PW 1830 and driven by a computer, endowed with a software for powder X-ray diffractogram interpretations. The explored 2θ interval goes from 5° to 45° at a rate of 0.02° per second in order to determine the nature and the crystallinity percentage of the various phases [24]. The intensity of the peaks is evaluated by counts reported as an arbitrary unit. It is connected to the crystallinity of the bones. The number of counts gives a qualitative analysis of the crystallinity [23].

The specimens of graft are characterized by porosity and pore size distribution by mercury porosimetry utilizing a *Micrometrics Auto Pore IV*.

The scanning electron microscope (SEM) used is the Stereoscan 360S, totally controlled and driven by a computerised system (CPU 32 bits). The SEM microscope is equipped with an Energy Dispersive X-ray Analysis (EDAX) system. Magic angle spinning NMR spectra of ^{13}C and ^{31}P were carried out on a Bruker MSL 400 spectrometer. The ^{31}P-NMR (161.92 MHz) spectra were measured with a 2.5 μs (π/4) and a repetition time of 10.0 s, while the twelve ^{13}C-NMR (100.61 MHz) spectra were recorded with a 4.5 μs (π/2) pulse and a repetition time of 4.0 s in CP condition (contact time = 5.0 ms). The number of scans varied between 1,000 and 10,000 for ^{31}P-NMR spectra and between 8,000 and 16,000 for ^{13}C-NMR spectra [25, 26].

4. RESULTS AND DISCUSSION

4.1. CHARACTERISATION OF THE CONTROL TESTS

The XDR analysis was made on the bones of the forelimbs and posterior limbs of the rats. Figure 1 shows the XRD of the bone samples of the forelimbs and posterior limbs of the rats, related with a spectrum of pure hydroxyapatite (HPA) (Carlo Erba RPE)

The peaks are characteristic of the hydroxyapatite and the diffractogram spectra are identical for the bones of the forelimb and posterior limb. Indeed, as Fig. 1C shows, the spectra of Fig. 1A and B are similar to that of 100 % crystalline percentage hydroxyapatite.

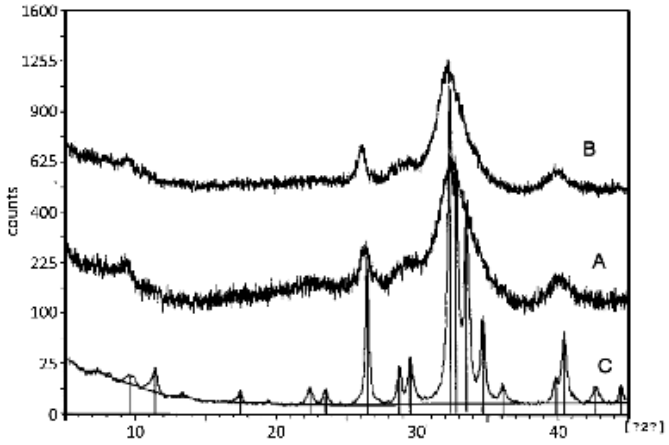

Fig. 1 – X-ray diffractograms of the bones of: A) forelimb; B) posterior limb of the rats; C) pure hydroxyapatite.

The amorphous matrix is attributed to organic substances, while the crystalline one is due to hydroxyapatite. Table 1 shows the 2θ values together with the *d*-spacing of pure hydroxyapatite and of the bones of forelimb and posterior limb.

Table 1

2θ and *d*-spacing data of pure hydroxyapatite and the control tests of bones of forelimb and posterior limb of the rats

Hydroxyapatite (100 %)		**Bones of forelimb (25 %)**		**Bones of posterior limb (32 %)**	
2θ	***d*-spacing**	**2θ**	***d*-spacing**	**2θ**	***d*-spacing**
9.325	9.4762	9.130	9.6781	9.055	9.7561
11.090	7.9717				
17.100	5.1811				
22.075	4.0234				
23.170	3.8357				
26.135	**3.4068**	26.060	3.4165	26.355	3.3789
28.400	3.1401				
29.185	3.0574				
32.050	**2.7903**	32.085	2.7873	32.315	2.7680
32.405	2.7605				
33.160	2.6994				
34.305	2.6119				
35.720	2.5116				
39.470	2.2814				
40.080	**2.2478**	39.885	2.2584	40.040	2.2500
42.260	2.1368				
44.070	2.0531				

The bone of the forelimb of the rat contains about 15–25 % crystalline regions. The various differences are correlated with the initial weight of each sample as it is shown in Fig. 2. It is clearly shown that the crystallinity increases as a function of increasing initial weight of the bones.

Although the experimental points are rather scattered, it can be concluded that, for the same initial weight, the crystallinity is higher for the bones of the posterior limbs. This is due to a higher hydroxyapatite content that increases the mechanical resistance of the limbs. Indeed, the use of the posterior limb is more accentuated in the rats. They have to respond at a higher stimulation with respect to the forelimbs.

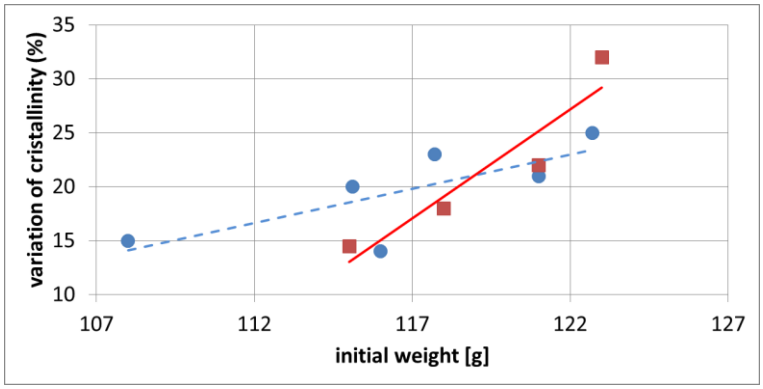

Fig. 2 – Variation of the crystallinity percentage of the bones as a function of their initial weight: of the forelimb (circle and dotted line), and of posterior limb (square and full line).

4.2. CHARACTERISATION OF THE GRAFTED RAT BONES

The rat bone samples were grafted with a pastille of MCPM and CC powder. Figure 3 shows the XRD spectra of the prepared pastille (black line) and graft extracted from the sample (grey line). The spectrum is rather different from that of pure hydroxyapatite. After about one month the pastille was extracted from samples and the XRD analysis was carried out. It is obvious that the diffractogram of the extracted pastille is more similar to that of the rat bones (Fig. 1 A, B) than to that of pure hydroxyapatite (Fig. 1 C).

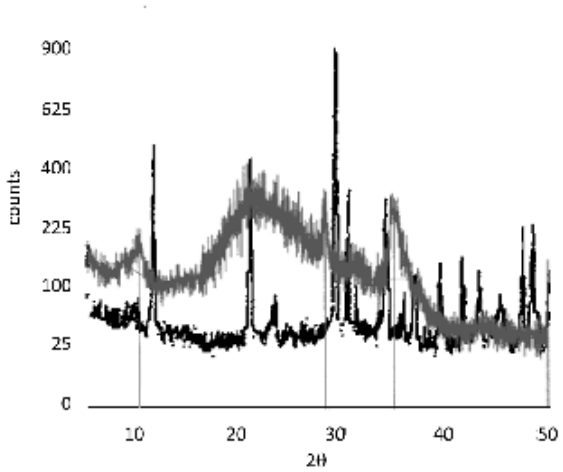

Fig. 3 – XR diffractogram of the: MCPM/CC pastille (black line) and graft extracted from the sample (grey line).

The XRD shows clearly that the graft can be absorbed by the rat organism without any problem. In order to better emphasize this phenomenon, the crystallinity of the bones of the forelimbs and posterior limbs of the rat is plotted as a function of the initial weight of the bone (Fig. 4). These graphs are not different from those obtained in the control tests (Fig. 2). This shows clearly that the graft, although remaining in the body of the rat for several days, does not cause any decompensation in the rat metabolism.

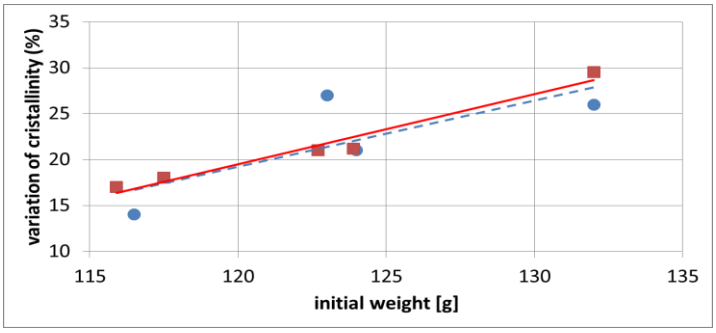

Fig. 4 – Variation of the crystallinity percentage of the bones as a function of initial weight of the bones in the case of: grafted forelimb (circle and dotted line) and posterior limb (square and full line) of the rat.

4.3. BONE CHARACTERISATION OF THE RAT TREATED IN A HYPERBARIC CHAMBER

The XRD analysis was also carried out on bone samples of the forelimb of the rat treated in a hyperbaric chamber. The hyperbaric oxygen therapy has led to an inversion of the relationship between the crystallinity percentage and the initial weight. Indeed, Fig. 5a, shows that the crystallinity percentage decreases as a function of increasing initial weight.

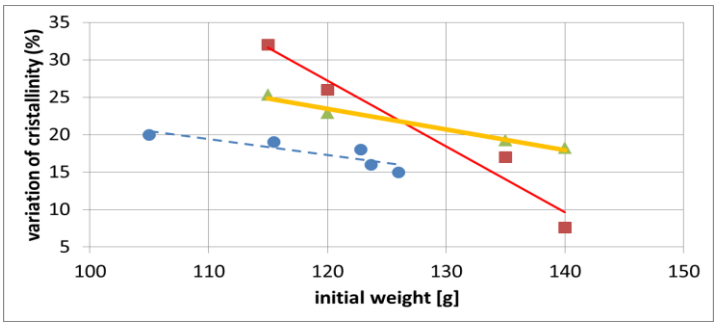

Fig. 5 – Variation of the crystallinity percentage as a function of initial weight of the bones of the: a) forelimb of the rat treated in a hyperbaric chamber (circle and dotted line); b) grafted forelimb of the rat treated in a hyperbaric chamber (square and full line); c) grafted posterior limb of the rat treated in a hyperbaric chamber (triangle and bold line).

The same inversion occurs in the grafted samples from the rat treated in a hyperbaric chamber (Fig. 5b), confirming again that the MCPM/CC pastille has no effect on the metabolism of the rat organism. The hyperbaric therapy is thus favouring the impoverishment of the bone crystalline phase.

The same behaviour is shown for the grafted posterior limb of the rat treated in a hyperbaric chamber. Fig. 5c shows the decrease of the crystallinity percentage of the grafted posterior limb of the rat treated in a hyperbaric chamber as a function at increasing initial bone weight.

In all the above mentioned cases, a better linear correlation is obtained (*i.e*. the experimental points are less scattered) when the rats are treated in a hyperbaric chamber. In these cases, the correlation becomes more evident as it is shown in Table 2 where the parameters are satisfying for the equation, $y = a + bx$, with the regression coefficient r.

4.4. MORPHOLOGICAL STUDY OF THE RAT BONES

The morphology of the rat bones is studied by SEM. Figure 6a shows a fragment of the forelimb bone of the rat where the filamentous form, characteristic of the collagen, is clearly seen embedded in the organic matrix.

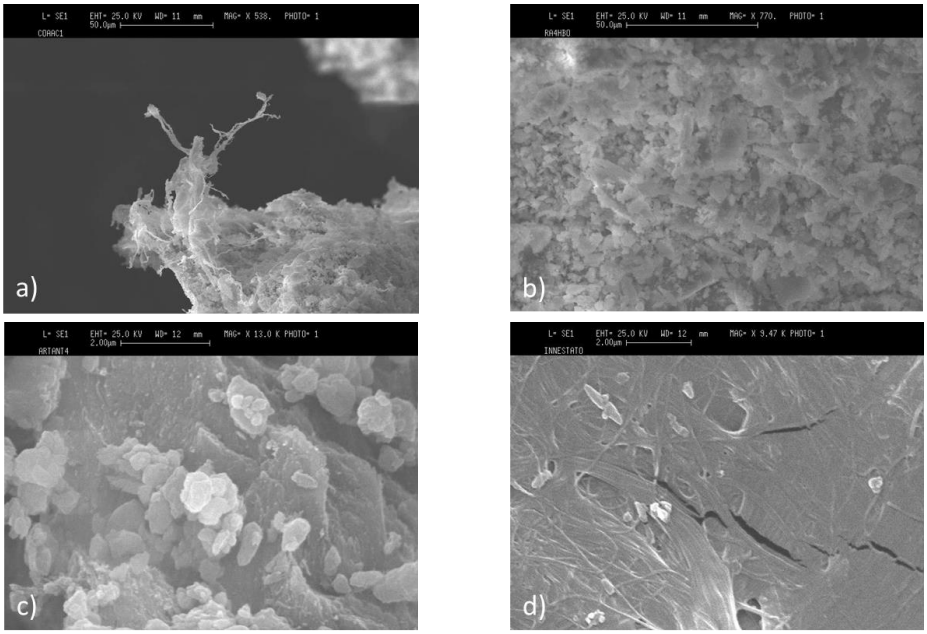

Fig. 6

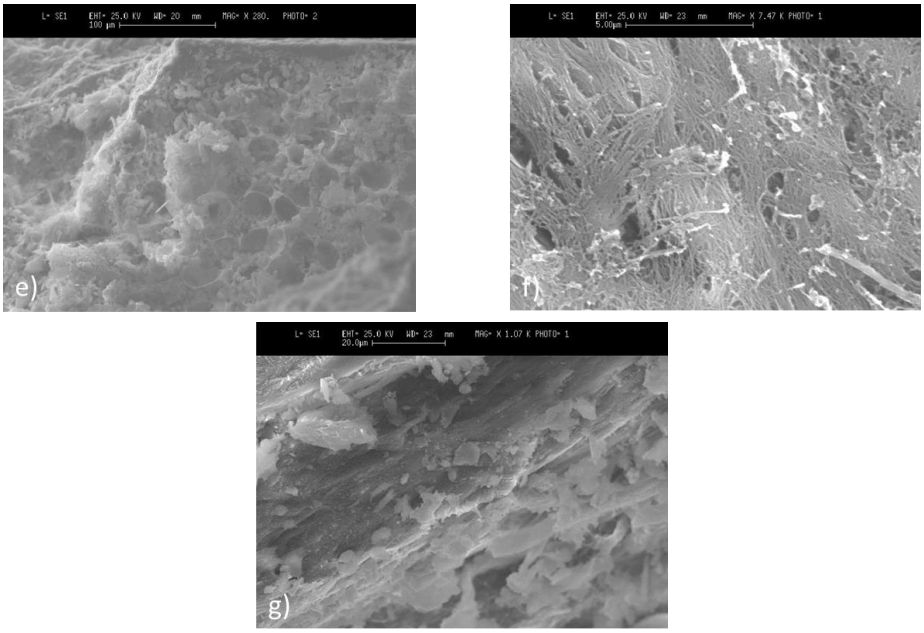

Fig. 6 (continued) – SEM picture of:
a) control test of forelimb of the rat;
b) bone of forelimb of the rat treated in a hyperbaric chamber;
c) grafted bone of forelimb of the rat;
d) surface of the MCPM/CC pastille extracted from the rat;
e) grafted bones of forelimb picture of the rat treated in a hyperbaric chamber;
f) bone of posterior limb of the rat;
g) grafted bone of posterior limb.

Figure 6b shows the SEM image of the bone of forelimb of the rat treated in a hyperbaric chamber. The morphology is compact and no particular details can be revealed. One can however, notice some filaments of collagen. In Fig. 6c one can see the compactness of the forelimb bone of a rat grafted with a MCPM/CC pastille. The slight variation in the morphology probably stems from the greater calcification of the bones due to the presence of the graft. Figure 6d illustrates the morphology of the graft after resection from the limb of the rat. Its surface is regular and smooth. The filaments are remembering of those of collagen. Figure 6e shows the morphology of the grafted forelimb bones of the rat treated in a hyperbaric chamber. One can notice the presence of very small hydroxyapatite crystals. Figure 6f shows the bone samples of the posterior limb of the rat used as a control test. One can see much better the presence of collagen filaments. The internal surface is more regular, although the rugosity increases due to the interwoven nature of the structure. Figure 6g shows the surface of a bone of posterior limb from a grafted rat. Its morphology is similar to that of grafted bone

of forelimb. This shows once again the increase of compactness of the bone after grafting.

4.5. NMR ANALYSIS OF THE SAMPLES

A typical magic angle spinning high resolution solid state ^{31}P-NMR spectrum is shown in Fig. 7. The maximum of the main NMR line is at 2.9 ppm with respect to aqueous H_3PO_4 and is characteristic of the hydroxyapatite in the bone tissue [5]. The NMR line can be decomposed into a narrow line (linewidth at half height 450 Hz) and a broad line (linewidth of about 1,000 Hz). Note that the linewidth of the narrow line is still broader than the pure hydroxyapatite (about 60 Hz [5]).

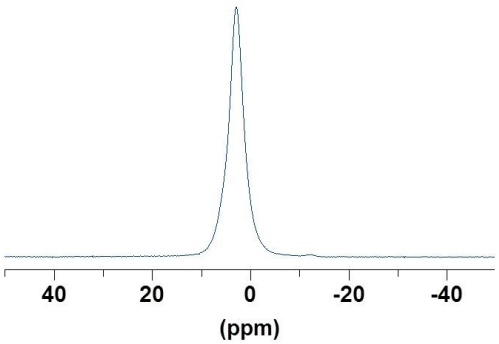

Fig. 7 – Magic angle spinning ^{31}P-NMR spectrum of a control test of the bone of the rat posterior limb.

The difference between different samples stems from the partial amorphous nature the bone components. Indeed, the crystallinity arises only at about 20 %. The ^{31}P-NMR spectra of all the samples studied (Table 2) are similar showing that the nature of the bone remains the same despite the variation of the crystallinity.

Table 2

Parameters of the equation, $y = a + bx$, together with the regression coefficient, r, for the crystallinity percentage correlation of the bones with the initial weight of the bones, HBC = hyperbaric chamber

Sample	Figure	*a*	*b*	*r*
Control forelimb	3	–54.1	0.63	0.762
Control posterior limb	3	12.6	0.06	0.069
Grafted forelimb	6	–65.5	0.71	0.779
Grafted posterior limb	7	–69.5	0.74	0.978
HBC forelimb	8	42.7	–0.02	–0.876
Grafted + HBC forelimb	9	131.0	–0.87	–0.980
Grafted + HBC posterior limb	10	55.2	–0.26	–0.986

Figure 8 shows the typical magic angle spinning (MAS) ^{13}C-NMR of a bone sample. One can notice that all the spectra are identical. It is easy to recognize the components of the collagen, *e.g.* the amide-groups centred on the 170 ppm, the proline components at 60, 46, 30 and 24 ppm, the glycine component at 50 ppm [25].

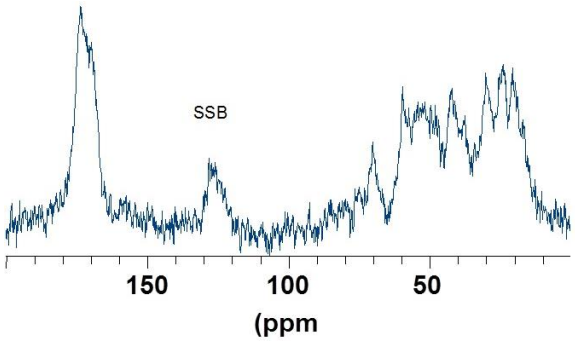

Fig. 8 – Magic angle spinning ^{13}C-NMR spectrum of posterior limb of control.

5. CONCLUSIONS

The X-ray diffraction was made on the bones of the forelimbs and posterior limbs of the rat demonstrating that their crystalline matrix is due to hydroxyapatite. The bone crystallinity increases as a function of increasing initial weight of bones. The crystallinity is higher for the bones of the posterior limbs.

The crystallinity of grafted rat bones of the forelimbs and posterior limbs is not different from those obtained in the control tests. This shows that the graft does not cause any decompensation in the rat metabolism. The hyperbaric therapy has led to an inversion of the relationship between the crystallinity percentage and the initial weight in the treated samples, as well as compared to the control samples. The same inversion occurs in the grafted samples treated in hyperbaric chamber.

The graft determines the compactness of the bone. Morphology of samples harvested from the rats treated in hyperbaric chamber is similar to that of controls. The ^{31}P-NMR spectra of all the samples are similar, showing that the nature of the bone remains the same despite the variation of the crystallinity.

The MAS ^{13}C-NMR spectra of all samples are identical.

Acknowledgements. This work was partially supported by the Italian Grant RIDITT project DI.TR.IM.MIS "Diffusion and transfer of technologies to companies working in the field of measurement", funded by the Italian Minister of Economic Development (MISE). The authors are indebted to Mr. Guy Daelen and to J.B. Nagy for recording the NMR spectra and preparing the corresponding figures, and to D. Vuono for taking the XRD spectra and SEM pictures.

REFERENCES

1. G. Treccani, *Fisiologia del sistema osseo*, in: *Sistema osseo. Enciclopedia Italiana*, Istituto Poligrafico dello stato, Roma, **25**, 703 (1946).
2. P. Rosati, *Citologia Istologia*, Edi-Ermes. Milano, 1989, pp. 657-672.
3. Jae-Young Rho, Liisa Kuhn-Spearing, Peter Zioupos, *Mechanical properties and the hierarchical structure of bone*, Medical Engineering & Physics **20**, 92-102 (1998).
4. J. Timonen, L. Alvila, P. Hirva, T.T. Pakkanen, *Nuclear magnetic renonance imaging a potential method for analysis of bone material*, Journal of Materials Science: Materials in Medicine **9**, 187-190 (1998).
5. A.P. Legrand, H. Sfihi, and J.M. Bouler, *Nuclear Magnetic Resonance Spectroscopy of Bone Substitutes*, Bone **25**, *2*, 103S-105S (1999).
6. D.L. Carnì, D. Grimaldi, F. Lamonaca, *Image pre-processing for micro nucleuses detection in lymphocyte*, IEEE International Workshop on *Intelligent Data Acquisition and Advanced Computing Systems: Technology and Applications*, Sofia, Bulgaria, 5-7 September 2005, pp. 570-575. DOI: 10.1109/IDAACS.2005.283048.
7. Y. Kurylyak, F. Lamonaca, D. Grimaldi, *A Neural Network-based Method for Continuous Blood Pressure Estimation from a PPG Signal*, IEEE International Instrumentation and Measurement Technology Conference (I2MTC 2012), Minnesota, USA, 6-9 May, 2013, pp. 280-283. DOI: 10.1109/I2MTC.2013.6555424.
8. Y. Kurylyak, F. Lamonaca, G. Mirabelli, *Detection of the Eye Blinks for Human's Fatigue Monitoring*, IEEE International Workshop on *Medical Measurements and Applications* (MeMeA 2012), Budapest, Hungary, 18-19 May 2012, pp. 91-94. DOI: 10.1109/MeMeA.2012.6226666.
9. D. Grimaldi, F. Lamonaca, C. Macrì, *Reduction of Doubtful Detection of Human Lymphocyte Micro-Nucleus Based on Wiener's Deconvolution and Computing Distributed Service*, IEEE International Workshop on *Medical Measurements and Applications* (MeMeA 2008), Ottawa, Ontario, Canada, 9-10 May 2008, pp. 114-119. DOI: 10.1109/MEMEA.2008.4543010.
10. K. Barbè, Y. Kurylyak, F. Lamonaca, *Logistic ordinal regression for the calibration of oscillometric blood pressure monitors*, Biomedical Signal Processing & Control **11**, 89–96, 2014,. DOI:10.1016/j.bspc.2014.01.012,
11. R. Morello, C. De Capua, F. Lamonaca, M.G. Belvedere, *Experimental Validation of Revised Criteria for Pulmonary Hypertension Diagnosis by Uncertainty Evaluation*, Transaction on Instrumentation and Measurement **63**, *3*, pp. 592-602 (2014). DOI: 10.1109/TIM.2013.2281559.
12. M. Ceccarelli, D. Grimaldi, F. Lamonaca, *Automatic Detection and Surface Measurement of Micronucleus by a Computer Vision Approach*, IEEE Transaction on Instrumentation and Measurement **59**, *9*, 2383-2390 (2010). DOI: 10.1109/TIM.2010.2049184.
13. D.L. Carnì, D. Grimaldi, F. Lamonaca, *Preprocessing Correction for Micronucleus Image Detection Affected by Contemporaneous Alterations*, IEEE Transaction on Instrumentation and Measurement **56**, *4*, 1202-1211 (2007).
14. D. Grimaldi, F. Lamonaca, *Reduction of doubtful detection of micro-nucleus in human lymphocyte*, Int. J. Advanced Media and Communication **3**, *1/2*, 80-94 (2009).
15. F. Lamonaca, E. Santoro, V. Spagnuolo, D. Grimaldi, *Clinical Investigation on the use of smartphone for oxygen saturation measurement*, Italian Journal of Medicine **9**, Suppl. 2, p. 56 (2015).
16. F. Lamonaca, K. Barbè, G. Polimeni, D. Grimaldi, *Health parameters monitoring by smartphone for quality of life improvement measurement*, Measurement **73**, *28*, 82-94 (2015).
17. S. Bohic, C. Rey, A. Legrand, H. Sfihi, R. Rohanizadeh, C. Martel, A. Barbier, and G. Daculsi, *Characterization of the Trabecular Rat Bone Mineral: Effect of Ovariectomy and Bisphosphonate Treatment*, Bone **26**, *4*, 341-348 (2000).

18. F. Lamonaca, M. Vasile, L.M. Caligiuri, A. Nastro, *Measurement method based on thermal analysis for the characterization of frozen and banked human bones*, World Journal of Engineering **11**, *6*, 621-626 (2014).
19. F. Lamonaca, L.M. Caligiuri, M. Riccio, M. Vasile, A. Nastro, *Measurement Techniques for the Objective Diagnosis of Primary Gonarthrosis*, International Journal of Biology and Biomedical Engineering **8**, 184-190 (2014).
20. F. Lamonaca, M. Vasile, A. Nastro, *Hallux valgus: Measurements and characterization*, Measurement **57**, 97-101 (2014).
21. Kurian Jonesa, A. Wayne Evansb, R.G. Bristowa, Wilfred Levina, *Treatment of radiation proctitis with hyperbaric oxygen*, Radiotherapy and Oncology **78**, 91–94 (2006).
22. A.R. Calafiori, G. Di Marco, G. Martino, M. Marotta, *Preparations and characterization of calcium phosphate biomateriale*, J. Mat. Sci.: Mat. Med. **18**, *12*, 2331-2338 (2007).
23. http:\\www.dst.unipi.it/dst/berti/diffrattometria.htm
24. International Center for Diffraction Data, *Tables* 9-390, 9-347, 5-0586, 9-432 (1987).
25. E. Breitmeier, W. Voelter, Carbon-13 NMR Spectroscopy, High-Resolution Methods and Applications in Organic Chemistry and Biochemistry, Third, completely revised edition, VCH, Weinheim, pp. 415-419 (1990).
26. D. Grimaldi, M. Marinov, *Distributed measurement systems*, Measurement: Journal of the International Measurement Confederation **30**, *4*, 279-287 (2001).